Letter

# Probing neutral triple gauge couplings with $Z^*\gamma$ ($\nu\bar{\nu}\gamma$) production at hadron colliders

John Ellis,[1,*] Hong-Jian He,[2,†] and Rui-Qing Xiao[3,‡]

[1]*Department of Physics, King's College London, Strand, London WC2R 2LS, United Kingdom; Theoretical Physics Department, CERN, CH-1211 Geneva 23, Switzerland; and T. D. Lee Institute, Shanghai Jiao Tong University, Shanghai, China*

[2]*T. D. Lee Institute and School of Physics and Astronomy, Key Laboratory for Particle Astrophysics and Cosmology, Shanghai Key Laboratory for Particle Physics and Cosmology, Shanghai Jiao Tong University, Shanghai, China; Physics Department and Institute of Modern Physics, Tsinghua University, Beijing, China; and Center for High Energy Physics, Peking University, Beijing, China*

[3]*Department of Physics, King's College London, Strand, London WC2R 2LS, United Kingdom and T. D. Lee Institute and School of Physics and Astronomy, Shanghai Jiao Tong University, Shanghai, China*

(Received 8 September 2023; accepted 8 November 2023; published 28 December 2023)

We study probes of neutral triple gauge couplings (nTGCs) via $Z^*\gamma$ production with off-shell decays $Z^* \to \nu\bar{\nu}$ at the LHC and the projected $pp$ (100 TeV) colliders, including both $CP$-conserving (CPC) and $CP$-violating (CPV) couplings. We present the dimension-8 Standard Model effective field theory (SMEFT) operators contributing to nTGCs and derive the correct form factor formulation for the doubly off-shell vertices $Z^*\gamma V^*$ $(V = Z, \gamma)$ by matching them with the dimension-8 SMEFT operators. We include new contributions enhanced by the large off-shell momentum of $Z^*$, beyond those of the conventional $Z\gamma V^*$ vertices with on-shell $Z\gamma$. We analyze the sensitivity reaches for probing the CPC/CPV nTGC form factors and the new physics scales of the dimension-8 nTGC operators at the LHC and future 100 TeV $pp$ colliders. We compare our new predictions with the existing LHC measurements of CPC nTGCs in the $\nu\bar{\nu}\gamma$ channel and demonstrate the importance of our new method.

DOI: 10.1103/PhysRevD.108.L111704

*Introduction.* Neutral triple gauge couplings (nTGCs) are attracting increased theoretical and experimental interest [1–6]. This is largely driven by the fact [7,8] that the nTGCs do not appear in the Standard Model (SM) Lagrangian, nor do they show up in the dimension-six Lagrangian of the SM effective field theory (SMEFT) [9]; hence, they could open up a unique window to the new physics beyond the SM that may first appear at the dimension-8 level. There have been extensive studies of the dimension-six operators [9–11] in the SMEFT, which do not involve nTGCs because they first appear as a set of dimension-8 operators. For probing nTGCs through the reaction $f\bar{f} \to Z\gamma$, the previous literature mainly focused on $CP$-conserving (CPC) nTGCs. For $e^+e^-$ colliders, on-shell $Z\gamma$ production with $Z \to \ell^+\ell^-$, $\nu\bar{\nu}, q\bar{q}$ have been considered, but at $pp$ colliders off-shell decays $Z^* \to \nu\bar{\nu}$ cannot be separated from on-shell invisible $Z$ decays because of the insufficient kinematic information of $Z$. Hence, it is important to study the off-shell production of $Z^* \to \nu\bar{\nu}$ at $pp$ colliders.

In this Letter, we study the doubly off-shell neutral triple gauge vertices (nTGVs) $Z^*\gamma V^*$ $(V = Z, \gamma)$ and present a new analysis including both the CPC and $CP$-violating (CPV) nTGCs. We first formulate the correct CPC and CPV form factors of $Z^*\gamma V^*$ vertices that are compatible with the full electroweak gauge symmetry $\mathrm{SU}(2) \otimes \mathrm{U}(1)$ of the SM [12]. By matching the CPC and CPV dimension-8 nTGC operators with the nTGC form factors, we derive the correct formulations of the $Z^*\gamma V^*$ form factors. Then, we study the sensitivity reaches of the LHC and the projected 100 TeV $pp$ colliders for probing the CPC/CPV nTGCs via the reaction $pp(q\bar{q}) \to Z^*\gamma \to \nu\bar{\nu}\gamma$. We further compare our new predictions with the existing LHC measurements [5] of CPC nTGCs in the $\nu\bar{\nu}\gamma$ channel and demonstrate the importance of using our new nTGC form factor formulation for the correct LHC analysis.

*Corresponding author: john.ellis@cern.ch
†Corresponding author: hjhe@sjtu.edu.cn
‡Corresponding author: xiaoruiqing@sjtu.edu.cn

*Formulating $Z^*\gamma V^*$ form factors from matching the SMEFT.* Our previous works [1–3] studied the dimension-eight SMEFT operators that generate the CPC nTGCs and their contributions to the on-shell $Z\gamma$ production at the LHC and future colliders. However, unlike the case of $e^+e^-$ collisions where the on-shell constraint can be imposed on the invisible decays $Z \to \nu\bar{\nu}$, this is not possible in $pp$ collisions, for which only the missing transverse momentum can be measured. Moreover, since $Z$ is an unstable particle, the invariant masses of $\ell^+\ell^-$ and $q\bar{q}$ final states from $Z$ decays are not exactly on shell in general. Hence, it is important to study the nTGVs with the final-state $Z^*$ off shell.

The general dimension-8 SMEFT Lagrangian takes the form

$$\mathcal{L}_8 = \sum_j \frac{\tilde{c}_j}{\tilde{\Lambda}^4}\mathcal{O}_j = \sum_j \frac{\mathrm{sign}(\tilde{c}_j)}{\Lambda_j^4}\mathcal{O}_j = \sum_j \frac{1}{[\Lambda_j^4]}\mathcal{O}_j, \quad (1)$$

where the dimensionless coefficients $\tilde{c}_j$ may take either sign, $\mathrm{sign}(\tilde{c}_j) = \pm$. For each dimension-8 operator $\mathcal{O}_j$, we define in Eq. (1) the corresponding effective cutoff scale for new physics, $\Lambda_j \equiv \tilde{\Lambda}/|\tilde{c}_j|^{1/4}$, and introduce the notation $[\Lambda_j^4] \equiv \mathrm{sign}(\tilde{c}_j)\Lambda_j^4$.

The following CPC and CPV nTGC operators include Higgs doublets:

$$\mathcal{O}_{\tilde{B}W}^{(\mathrm{CPC})} = iH^\dagger \tilde{B}_{\mu\nu} W^{\mu\rho}\{D_\rho, D^\nu\}H + \mathrm{H.c.}, \quad (2a)$$

$$\mathcal{O}_{\widetilde{BW}}^{(\mathrm{CPC})} = iH^\dagger \left(D_\sigma \widetilde{W}^a_{\mu\nu} W^{a\mu\sigma} + D_\sigma \tilde{B}_{\mu\nu} B^{\mu\sigma}\right) D^\nu H + \mathrm{H.c.}, \quad (2b)$$

$$\tilde{\mathcal{O}}_{BW}^{(\mathrm{CPV})} = iH^\dagger B_{\mu\nu} W^{\mu\rho}\{D_\rho, D^\nu\}H + \mathrm{H.c.}, \quad (2c)$$

$$\tilde{\mathcal{O}}_{WW}^{(\mathrm{CPV})} = iH^\dagger W_{\mu\nu} W^{\mu\rho}\{D_\rho, D^\nu\}H + \mathrm{H.c.}, \quad (2d)$$

$$\tilde{\mathcal{O}}_{BB}^{(\mathrm{CPV})} = iH^\dagger B_{\mu\nu} B^{\mu\rho}\{D_\rho, D^\nu\}H + \mathrm{H.c.}, \quad (2e)$$

where $H$ denotes the SM Higgs doublet. The operators (2a) and (2c)–(2e) were given in [8], to which we have further added an independent CPC operator (2b). For the dimension-eight CPC and CPV nTGC operators containing pure gauge fields only, we have

$$g\mathcal{O}_{G+}^{(\mathrm{CPC})} = \tilde{B}_{\mu\nu} W^{a\mu\rho}\left(D_\rho D_\lambda W^{a\nu\lambda} + D^\nu D^\lambda W^a_{\lambda\rho}\right), \quad (3a)$$

$$g\mathcal{O}_{G-}^{(\mathrm{CPC})} = \tilde{B}_{\mu\nu} W^{a\mu\rho}\left(D_\rho D_\lambda W^{a\nu\lambda} - D^\nu D^\lambda W^a_{\lambda\rho}\right), \quad (3b)$$

$$g\tilde{\mathcal{O}}_{G+}^{(\mathrm{CPV})} = B_{\mu\nu} W^{a\mu\rho}\left(D_\rho D_\lambda W^{a\nu\lambda} + D^\nu D^\lambda W^a_{\lambda\rho}\right), \quad (3c)$$

$$g\tilde{\mathcal{O}}_{G-}^{(\mathrm{CPV})} = B_{\mu\nu} W^{a\mu\rho}\left(D_\rho D_\lambda W^{a\nu\lambda} - D^\nu D^\lambda W^a_{\lambda\rho}\right), \quad (3d)$$

where the operators $(\mathcal{O}_{G+}, \mathcal{O}_{G-})$ are CPC [2], and the two new CPV operators $(\tilde{\mathcal{O}}_{G+}, \tilde{\mathcal{O}}_{G-})$ are constructed. The operators (2) and (3) belong to two classes, $F^2\phi^2D^2$ and $F^3D^2$. From the classification of [13] the relevant dimension-eight operators contain $F^2H^2D^2$, $F^2\psi^2D$, and $F^4$, where $F^2\psi^2D$ and $F^4$ do not explicitly contain any nTGC vertices and thus are not included here (see Supplemental Material [14]). Using integration by parts and equations of motion, we find that the $F^3D^2$ type can be converted into three types of operators $(F^4, F^2\psi^2D, F^2H^2D^2)$, where $F^2H^2D^2$ corresponds to our Eq. (2). Moreover, the $F^2H^2D^2$ type of Eq. (2) contributes to the form factors $(h_3^V, h_1^V)$ only, but not to $(h_4^V, h_2^V)$, as shown by Eqs. (6) and (8) below. Hence, the operator types $F^2\phi^2D^2$ and $F^3D^2$ provide the optimal basis for the current nTGC study [14].

The conventional formalism for nTGC form factors was proposed over 20 years ago [7] and respects only the residual gauge symmetry $\mathrm{U}(1)_{\mathrm{em}}$. However, as we stressed [1], it does not respect the full electroweak gauge symmetry $\mathrm{SU}(2) \otimes \mathrm{U}(1)$ of the SM and leads to large unphysical high-energy behaviors of certain scattering amplitudes [1]. We thus proposed [1] a new formulation of the CPC form factors of the nTGVs $Z\gamma V^*$ that is compatible with the full SM gauge group with spontaneous electroweak symmetry breaking. We will construct an extended formulation to include the CPV nTGVs for this study.

The doubly off-shell nTGC form factors for $Z^*\gamma V^*$ vertices are more complicated than that of $Z\gamma V^*$. Matching with the dimension-8 nTGC operators of the SMEFT, we parametrize the $Z^*\gamma V^*$ vertices as follows:

$$V^{\alpha\beta\mu}_{Z^*\gamma V^*} = \Gamma^{\alpha\beta\mu}_{Z^*\gamma V^*} + \frac{e}{M_Z^2} q_1^\alpha X^{\beta\mu}_{1V} + \frac{e}{M_Z^2} q_3^\mu X^{\alpha\beta}_{3V}, \quad (4)$$

where expressions for $X^{\beta\mu}_{1V}$ and $X^{\alpha\beta}_{3V}$ are given in the Supplemental Material [14] and we find that they have vanishing contributions to the processes $f\bar{f} \to Z^{(*)}\gamma$ with $Z^{(*)} \to f'\bar{f}'$. Hence, the present analysis only involves the vertices $\Gamma^{\alpha\beta\mu}_{Z^*\gamma V^*}$.

We first present the CPC parts of the $\Gamma^{\alpha\beta\mu}_{Z^*\gamma V^*}$ vertices,

$$\Gamma^{\alpha\beta\mu}_{Z^*\gamma\gamma^*}(q_1,q_2,q_3) = \frac{e}{M_Z^2}\left(h_{31}^\gamma + \frac{\hat{h}_3^\gamma q_1^2}{M_Z^2}\right) q_3^2 q_{2\nu}\epsilon^{\alpha\beta\mu\nu} + \frac{e s_W \hat{h}_4 q_3^2}{2c_W M_Z^4}\left(2q_2^\alpha q_{3\nu} q_{2\sigma}\epsilon^{\beta\mu\nu\sigma} + q_3^2 q_{2\nu}\epsilon^{\alpha\beta\mu\nu}\right), \quad (5a)$$

$$\Gamma^{\alpha\beta\mu}_{Z^*\gamma Z^*}(q_1,q_2,q_3) = \frac{e(q_3^2 - q_1^2)}{M_Z^2}\left[\hat{h}_3^Z q_{2\nu}\epsilon^{\alpha\beta\mu\nu} + \frac{\hat{h}_4}{2M_Z^2}\left(2q_2^\alpha q_{3\nu} q_{2\sigma}\epsilon^{\beta\mu\nu\sigma} + q_3^2 q_{2\nu}\epsilon^{\alpha\beta\mu\nu}\right)\right]. \quad (5b)$$

In the above, we use the hat symbol to distinguish off-shell form factors $(\hat{h}_3^Z, \hat{h}_3^\gamma, \hat{h}_4)$ from their on-shell counterparts $(h_3^\gamma, h_3^Z, h_4)$ [1]. The CPC form factors $(h_{31}^\gamma, \hat{h}_3^\gamma, \hat{h}_3^Z, \hat{h}_4)$ can be mapped precisely to the cutoff scales $(\Lambda_{\widetilde{BW}}, \Lambda_{\tilde{B}W}, \Lambda_{G-}, \Lambda_{G+})$ of the dimension-8 operators $(\mathcal{O}_{\widetilde{BW}}, \mathcal{O}_{\tilde{B}W}, \mathcal{O}_{G+}, \mathcal{O}_{G-})$ as

$$\hat{h}_4 = -\frac{v^2 M_Z^2}{s_W c_W [\Lambda_{G+}^4]}, \qquad \hat{h}_3^Z = \frac{v^2 M_Z^2}{2 s_W c_W [\Lambda_{\tilde{B}W}^4]},$$
$$\hat{h}_3^\gamma = -\frac{v^2 M_Z^2}{2 c_W^2 [\Lambda_{G-}^4]}, \qquad h_{31}^\gamma = -\frac{v^2 M_Z^2}{s_W c_W [\Lambda_{\widetilde{BW}}^4]}, \tag{6}$$

where $[\Lambda_j^4] \equiv \mathrm{sign}(\tilde{c}_j)\Lambda_j^4$. The above relations hold for any momentum $q_1$ of $Z^*$, and for $q_1^2 = M_Z^2$ the off-shell form factors $(\hat{h}_3^Z, \hat{h}_3^\gamma, \hat{h}_4)$ reduce to the on-shell cases $\hat{h}_4 = h_4$, $\hat{h}_3^Z = h_3^Z$, and $\hat{h}_3^\gamma + h_{31}^\gamma = h_3^\gamma$, where $h_{31}^\gamma$ is part of the on-shell form factor $h_{31}^\gamma = h_3^\gamma - \hat{h}_3^\gamma$ for $q_1^2 = M_Z^2$.

The new formulations of the off-shell nTGC form factors $Z^*\gamma V^*$ in Eq. (5) (CPC case) and in Eq. (7) (CPV case) were not given in the literature [1,3,7,8]. As we discuss in the next section, CMS [4] and ATLAS [5] measured the CPC nTGC form factors $(h_3^\gamma, h_4^V)$ via $pp(q\bar{q}) \to Z^*\gamma \to \nu\bar{\nu}\gamma$, but used the conventional CPC nTGC form factor of $Z\gamma V^*$ with both $(Z, \gamma)$ assumed to be on shell [7]. Thus, their measurement of $h_3^\gamma$ is actually equivalent to measuring our form factor $h_{31}^\gamma$ in Eq. (5a) [15]. Hence the CMS and ATLAS analyses [4,5] missed the new form factor $\hat{h}_3^\gamma$ in Eq. (5a), whose contribution dominates over $h_{31}^\gamma$ in the $\nu\bar{\nu}\gamma$ channel for both the LHC and 100 TeV $pp$ colliders, as we demonstrate in the following section.

Next, using the Lagrangian of nTGVs as given by the dimension-8 nTGC operators [14] [cf. Eq. (S3) in the Supplemental Material], we construct the off-shell CPV nTGVs $\Gamma^{\alpha\beta\mu}_{Z^*\gamma V^*}$ as

$$\Gamma^{\alpha\beta\mu}_{Z^*\gamma\gamma^*}(q_1, q_2, q_3) = \frac{e}{M_Z^2}\left(h_{11}^\gamma + \frac{\hat{h}_1^\gamma q_1^2}{M_Z^2}\right) q_3^2 \left(q_2^\alpha g^{\mu\beta} - q_2^\mu g^{\alpha\beta}\right) + \frac{e s_W \hat{h}_2 q_3^2}{2 c_W M_Z^4}\left(q_1^2 q_2^\alpha g^{\mu\beta} - q_3^2 q_2^\mu g^{\alpha\beta}\right), \tag{7a}$$

$$\Gamma^{\alpha\beta\mu}_{Z^*\gamma Z^*}(q_1, q_2, q_3) = \frac{e(q_3^2 - q_1^2)}{M_Z^2}\left[\hat{h}_1^Z \left(q_2^\alpha g^{\mu\beta} - q_2^\mu g^{\alpha\beta}\right) + \frac{\hat{h}_2}{2M_Z^2}\left(q_1^2 q_2^\alpha g^{\mu\beta} - q_3^2 q_2^\mu g^{\alpha\beta}\right)\right], \tag{7b}$$

which have important differences from the conventional CPV nTGC form factors [7], as we explain in [14]. When the final-state $Z$ boson is on shell ($q_1^2 = M_Z^2$), the above off-shell form factors reduce to the on-shell ones $h_{11}^\gamma + \hat{h}_1^\gamma = h_1^\gamma$, $\hat{h}_1^Z = h_1^Z$, and $\hat{h}_2 = h_2$. In the on-shell limit, the on-shell amplitude $\mathcal{T}[Z_T\gamma]$ should satisfy the equivalence theorem [16], which puts nontrivial constraints on the structure of form factors, as shown in [14].

Then, we can match these CPV nTGC form factors to the dimension-8 gauge-invariant CPV operators (2) and (3) in the broken phase and derive the relations

$$\hat{h}_1^Z = \frac{v^2 M_Z^2}{4 c_W s_W}\left(\frac{c_W^2 - s_W^2}{[\Lambda_{WB}^4]} - \frac{c_W s_W}{[\Lambda_{WW}^4]} + \frac{4 c_W s_W}{[\Lambda_{BB}^4]}\right), \tag{8a}$$

$$h_{11}^\gamma = \frac{v^2 M_Z^2}{4 c_W s_W}\left(\frac{2 c_W s_W}{[\Lambda_{WB}^4]} - \frac{s_W^2}{[\Lambda_{WW}^4]} - \frac{4 c_W^2}{[\Lambda_{BB}^4]}\right), \tag{8b}$$

$$\hat{h}_1^\gamma = \frac{v^2 M_Z^2}{4 c_W^2 [\Lambda_{\tilde{G}-}^4]}, \qquad \hat{h}_2 = -\frac{v^2 M_Z^2}{2 s_W c_W [\Lambda_{\tilde{G}+}^4]}. \tag{8c}$$

We find that the Higgs-field-dependent CPV operators (2c)–(2e) can generate the form factors $(h_{11}^\gamma, h_1^Z)$, where $h_{11}^\gamma$ is part of the on-shell form factor $h_1^\gamma = h_{11}^\gamma + \hat{h}_1^\gamma$.

In summary, there are eight independent CPC and CPV form factors for the nTGVs $Z^*\gamma V^*$. These can be mapped to the four CPC operators in Eqs. (2a), (2b), (3a), and (3b) and the five CPV operators in Eqs. (2c)–(2e), (3c), and (3d) [17]. This is in contrast to the case of doubly on-shell vertices $Z\gamma V^*$, which only have six independent parameters because $h_{31}^\gamma + \hat{h}_3^\gamma = h_3^\gamma$ and $h_{11}^\gamma + \hat{h}_1^\gamma = h_1^\gamma$.

*Probing nTGCs with $Z^*\gamma(\nu\bar{\nu}\gamma)$ production at hadron colliders.* The invariant mass of $Z^{(*)} \to \nu\bar{\nu}$ decays cannot be measured in the reaction $pp(q\bar{q}) \to \nu\bar{\nu}\gamma$. Hence, analyzing the $\nu\bar{\nu}\gamma$ production with off-shell $Z^*$ decays is important for $pp$ colliders. The partonic cross section of $q\bar{q} \to Z^{(*)}\gamma$ can be expressed as

$$\sigma = \sum_{q,\bar{q}} \int \mathrm{d}x_1 \mathrm{d}x_2 \left[\mathcal{F}_{q/p}(x_1, \mu)\mathcal{F}_{\bar{q}/p}(x_2, \mu)\sigma_{q\bar{q}}(\hat{s}) + (q \leftrightarrow \bar{q})\right], \tag{9}$$

where the functions $(\mathcal{F}_{q/p}, \mathcal{F}_{\bar{q}/p})$ denote the parton distribution functions (PDFs) of the quark and antiquark in the proton beams, and $\hat{s} = x_1 x_2 s$ [18]. The PDFs depend on the factorization scale $\mu$, which is set to $\mu = \sqrt{\hat{s}}/2$ in our

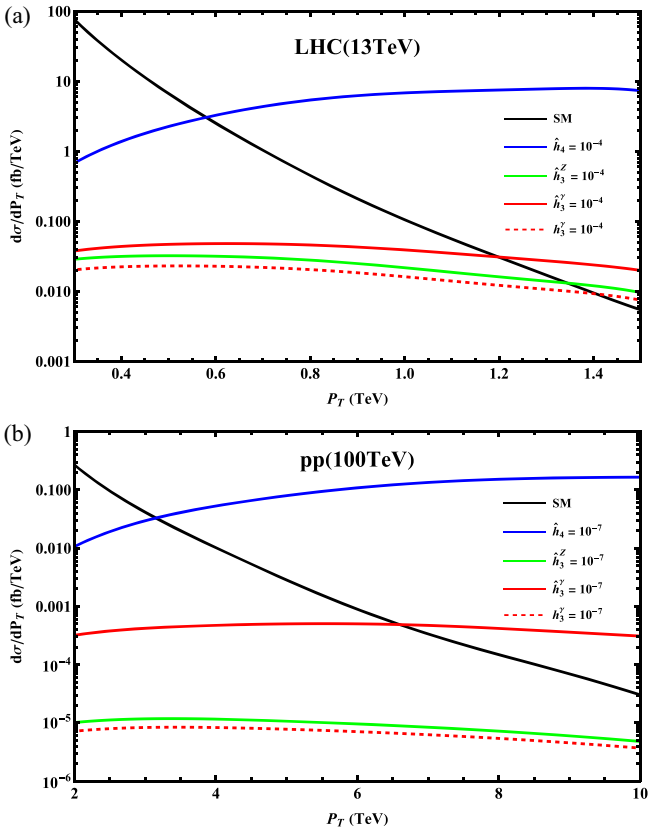


FIG. 1. Differential cross sections for $\nu\bar{\nu}\gamma$ production as functions of $P_T^\gamma$, shown in (a) for the LHC (13 TeV) and in (b) for the 100 TeV $pp$ collider. In each plot, the SM cross section is shown by a black curve, and the contributions of nTGC form factors are shown by colored curves.

analysis. We use the PDFs of the quarks $q = u, d, s, c, b$ and their antiquarks given by the CTEQ Collaboration [19].

We compute the partonic cross section in three parts,

$$\sigma(q\bar{q} \to Z^*\gamma) = \sigma_0 + \sigma_1 + \sigma_2, \tag{10}$$

where $\sigma_0$ is the SM contribution, $\sigma_1$ is the interference contribution between the nTGCs and the SM, and $\sigma_2$ is the squared nTGC contribution. The explicit formulas for $(\sigma_0, \sigma_1, \sigma_2)$ are given in the Supplemental Material [14]. The CPC and CPV amplitudes do not interfere for $q\bar{q} \to Z^{(*)}\gamma$, hence the contributions of the CPV nTGCs to $\sigma_1$ vanish. Moreover, we find $\sigma_1 \ll \sigma_2$ for the CPC nTGCs at the LHC and future $pp$ colliders, making $\sigma_1$ negligible in this analysis [20]. We further note that the contribution of each CPV nTGC to $\sigma_2$ has the same structure as that of the corresponding CPC nTGC.

For $\nu\bar{\nu}\gamma$ production, the photon's transverse momentum $P_T^\gamma$ is the major observable that can distinguish the new physics signals from the SM backgrounds. We present the $P_T^\gamma$ distributions of the $Z^*\gamma$ cross section for the LHC (13 TeV) in Fig. 1(a) and for the 100 TeV $pp$ collider in Fig. 1(b). In each plot, the contributions of the nTGC form factors $(\hat{h}_4, \hat{h}_3^Z, \hat{h}_3^\gamma, h_{31}^\gamma)$ (taking a reference value $10^{-4}$) are shown by the (blue, green, red, and red dashed) curves. We observe from Eq. (5a) that the $\hat{h}_3^\gamma$ contribution is strongly enhanced by the off-shell $Z^*$ momentum factor $q_1^2/M_Z^2$, whereas the $\hat{h}_{31}^\gamma$ contribution is not. Unlike $\hat{h}_3^\gamma$, this does not happen to $\hat{h}_3^Z$ because Eq. (5b) shows that the numerator factor $q_3^2 - q_1^2$ exhibits a strong cancellation between $q_3^2 (= \hat{s})$ and $q_1^2$ when $q_1^2$ goes far off shell. We find that the $\hat{h}_3^\gamma$ contribution (red solid curve) is larger than that of $\hat{h}_{31}^\gamma$ (red dashed curve) by about a factor of 2–3 for the LHC [Fig. 1(a)] and by a large factor (43–77) for the 100 TeV $pp$ collider [Fig. 1(b)]. The $\hat{h}_4$ contribution is much larger than that of $\hat{h}_3^Z$, $\hat{h}_3^\gamma$, and $h_{31}^\gamma$, because the $\hat{h}_4$ terms are enhanced by an extra large momentum factor of $q_2 q_3$ or $q_3^2$, as shown in Eq. (5).

To optimize the detection sensitivity, we divide events into bins of $P_T^\gamma$ distribution, whose widths we take as $\Delta P_T = 100$ GeV for the LHC and $\Delta P_T = 500$ GeV for the 100 TeV $pp$ collider. Then, we compute the significance $\mathcal{Z}_{\rm bin}$ for each bin and construct the following total significance measure:

$$\mathcal{Z}_{\rm total} = \sqrt{\sum \mathcal{Z}_{\rm bin}^2}. \tag{11}$$

Since the SM contribution $\sigma_0$ becomes small when the photon $P_T^\gamma$ is high, we determine the statistical significance for each bin by using the formula of the background-with-signal hypothesis [22],

$$\mathcal{Z} = \sqrt{2\left(\sigma_0 \ln\frac{\sigma_0}{\sigma_0 + \Delta\sigma} + \Delta\sigma\right)} \times \sqrt{\mathcal{L} \times \epsilon}, \tag{12}$$

where $\mathcal{L}$ is the integrated luminosity and $\epsilon$ denotes the detection efficiency. For our analysis, we choose an ideal detection efficiency $\epsilon = 100\%$ unless specified otherwise.

We present sensitivities for probing the CPC and CPV nTGC form factors $\hat{h}_j^V$ and the new physics scales $\Lambda_j$ of the dimension-8 nTGC operators in Tables I and II. For the LHC, we find that the sensitivities to $\hat{h}_2$ and $\hat{h}_4$ can reach $O(10^{-5}$–$10^{-6})$, whereas the sensitivities to $\hat{h}_{3,1}^Z$, $\hat{h}_{3,1}^\gamma$, and $h_{31,11}^\gamma$ are of $O(10^{-4})$. The sensitivities to $\hat{h}_j^V$ at the 100 TeV $pp$ collider are generally much higher than the LHC, by a factor of $O(10^2$–$10^3)$. The LHC sensitivities to $\hat{h}_{3,1}^\gamma$ are stronger than those to $h_{31,11}^\gamma$ and $\hat{h}_{3,1}^Z$ by about 50%–60%, whereas at the 100 TeV $pp$ colliders the sensitivities to $\hat{h}_{3,1}^\gamma$ are much higher than those to $h_{31,11}^\gamma$ and $\hat{h}_{3,1}^Z$, by factors of $O(10)$.

Both CMS (using 19.6/fb of run-1 data) [4] and ATLAS (using 36.9/fb of run-2 data) [5] measured the CPC nTGC

TABLE I. Sensitivity reaches on probing the CPC and CPV nTGC form factors at $2\sigma$ level, from analyzing the reaction $pp(q\bar{q}) \to Z^*\gamma \to \nu\bar{\nu}\gamma$ at the LHC (13 TeV) and the 100 TeV $pp$ collider, for each given integrated luminosity $\mathcal{L}$. In the second to last row, the $\hat{h}^\gamma_{3,1}$ sensitivities include the enhancement by off-shell effects, whereas the $h^\gamma_{31,11}$ in the last row do not.

| $\sqrt{s}$ | 13 TeV | | | | 100 TeV | | |
|---|---|---|---|---|---|---|---|
| $\mathcal{L}$ (ab$^{-1}$) | 0.14 | 0.3 | 3 | | 3 | 10 | 30 |
| $\lvert\hat{h}_{4,2}\rvert \times 10^6$ | 11 | 8.5 | 4.2 | $\lvert\hat{h}_{4,2}\rvert \times 10^9$ | 4.5 | 2.9 | 2.0 |
| $\lvert\hat{h}^Z_{3,1}\rvert \times 10^4$ | 2.2 | 1.7 | 0.90 | $\lvert\hat{h}^Z_{3,1}\rvert \times 10^7$ | 7.0 | 4.8 | 3.4 |
| $\lvert\hat{h}^\gamma_{3,1}\rvert \times 10^4$ | 1.6 | 1.3 | 0.67 | $\lvert\hat{h}^\gamma_{3,1}\rvert \times 10^7$ | 0.94 | 0.62 | 0.44 |
| $\lvert h^\gamma_{31,11}\rvert \times 10^4$ | 2.5 | 2.0 | 1.0 | $\lvert h^\gamma_{31,11}\rvert \times 10^7$ | 8.3 | 5.7 | 4.0 |

TABLE II. Sensitivity reaches on probing the new physics scales $\Lambda_j$ (in TeV) of the dimension-8 nTGC operators at $2\sigma$ level, as derived by analyzing the reaction $pp(q\bar{q}) \to Z^*\gamma \to \nu\bar{\nu}\gamma$ at the LHC (13 TeV) and at the 100 TeV $pp$ collider, with integrated luminosities $\mathcal{L}$ as indicated.

| $\sqrt{s}$ | 13 TeV | | | 100 TeV | | |
|---|---|---|---|---|---|---|
| $\mathcal{L}$ (ab$^{-1}$) | 0.14 | 0.3 | 3 | 3 | 10 | 30 |
| $\Lambda_{G+}$ (CPC) | 3.2 | 3.5 | 4.1 | 23 | 25 | 28 |
| $\Lambda_{G-}$ (CPC) | 1.2 | 1.3 | 1.5 | 7.7 | 8.5 | 9.3 |
| $\Lambda_{\tilde{B}W}$ (CPC) | 1.3 | 1.4 | 1.6 | 5.4 | 5.9 | 6.4 |
| $\Lambda_{\widetilde{BW}}$ (CPC) | 1.5 | 1.6 | 1.8 | 6.2 | 6.8 | 7.4 |
| $\Lambda_{\tilde{G}+}$ (CPV) | 2.7 | 2.9 | 3.5 | 19 | 21 | 23 |
| $\Lambda_{\tilde{G}-}$ (CPV) | 1.0 | 1.1 | 1.3 | 6.5 | 7.2 | 7.8 |
| $\Lambda_{WW}$ (CPV) | 0.93 | 1.0 | 1.2 | 3.9 | 4.3 | 4.6 |
| $\Lambda_{WB}$ (CPV) | 1.1 | 1.2 | 1.4 | 4.6 | 5.1 | 5.5 |
| $\Lambda_{BB}$ (CPV) | 1.3 | 1.4 | 1.7 | 5.6 | 6.2 | 6.8 |

form factors $(h^V_3, h^V_4)$ via the reaction $pp(q\bar{q}) \to Z^*\gamma \to \nu\bar{\nu}\gamma$; however, they used the conventional form factor formula for the doubly on-shell vertex $Z\gamma V^*$ [7]. This differs from our new formula of the doubly off-shell vertex $Z^*\gamma V^*$ in Eq. (5), which gives the correct nTGC form factor formulation for analyzing the $Z^*\gamma(\nu\bar{\nu}\gamma)$ production. For instance, using 36.1/fb of LHC run-2 data, ATLAS obtained the 95% C.L. bounds [5],

$$h^\gamma_3 \in (-3.7, 3.7) \times 10^{-4}, \quad h^Z_3 \in (-3.2, 3.3) \times 10^{-4},$$
$$h^\gamma_4 \in (-4.4, 4.3) \times 10^{-7}, \quad h^Z_4 \in (-4.5, 4.4) \times 10^{-7}. \quad (13)$$

For a quantitative comparison, we impose the same cut $P^\gamma_T > 600$ GeV as that of ATLAS [5] and choose a detection efficiency $\epsilon = 70\%$ [5]. We then derive the new LHC bounds (95% C.L.),

$$|h^\gamma_{31}| < 3.5 \times 10^{-4}, \quad |\hat{h}^\gamma_3| < 2.3 \times 10^{-4},$$
$$|\hat{h}^Z_3| < 3.1 \times 10^{-4}, \quad |\hat{h}_4| < 1.4 \times 10^{-5}. \quad (14)$$

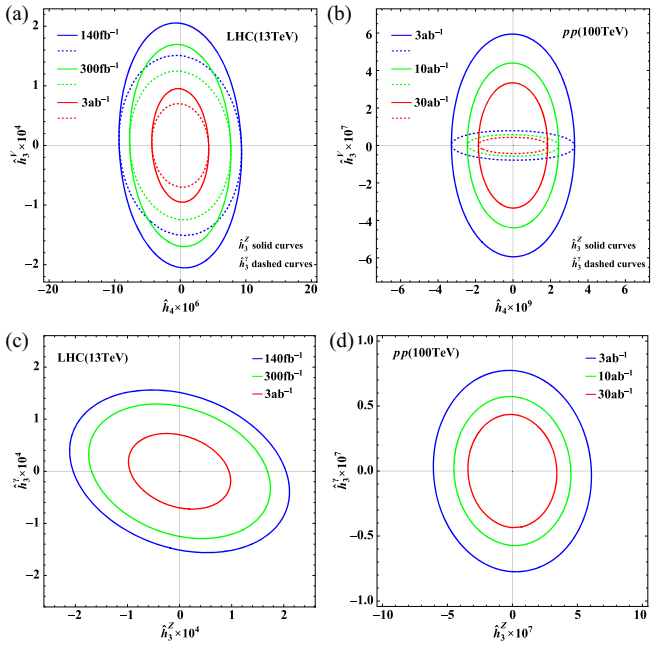


FIG. 2. Correlation contours (95% C.L.) for the sensitivities to each of the pairs of nTGC form factors at (a),(c) the LHC (13 TeV) and (b),(d) the 100 TeV $pp$ collider. (a),(b) Correlation contours for $(h_4, h^Z_3)$ (solid curves) and $(h_4, h^\gamma_3)$ (dashed curves). (c),(d) Depict the correlation contours for $(h^Z_3, h^\gamma_3)$.

Comparing our results (14) with the ATLAS result (13), we find that our bounds on $h^\gamma_{31}$ and $\hat{h}^Z_3$ agree well with the ATLAS bounds on $h^\gamma_3$ and $h^Z_3$ (to within a few percent), whereas our bound on $\hat{h}^\gamma_3$ is significantly stronger than the ATLAS bound on $h^\gamma_3$ by about 60%. This is because in our off-shell formulation of Eq. (5) the $\hat{h}^\gamma_3$ is enhanced by the $Z^*$ off-shell factor $q_1^2/M_Z^2$, but $h^\gamma_{31}$ and $\hat{h}^Z_3$ are not; thus their bounds are quite similar to the case of assuming on-shell invisible $Z$ decays. On the other hand, our $\hat{h}_4$ bound in Eq. (14) is much weaker than the ATLAS bounds on $(h^\gamma_4, h^Z_4)$, by a large factor of ~32, because the conventional nTGC form factor formulas are incompatible with the gauge-invariant SMEFT formulation of dimension eight (including spontaneous electroweak gauge symmetry breaking), as we explain in the Supplemental Material [14] and its Table S1. We emphasize that the existing ATLAS result [5] used the conventional on-shell nTGC formula of the vertex $Z\gamma V^*$ [7] for analyzing the $\nu\bar{\nu}\gamma$ channel, which caused a significant underestimate of the sensitivity to $\hat{h}^\gamma_3$ by about 60%. This underlines the importance for the ongoing LHC experimental analyses to use our *correct* theoretical formulation to analyze the $\nu\bar{\nu}\gamma$ channel for probing the nTGCs.

In Table II we demonstrate that the sensitivities to new physics scales in the coefficients of $\mathcal{O}_{G+}$ and $\tilde{\mathcal{O}}_{G+}$ can reach (2.7–4.1) TeV at the LHC and (19–28) TeV at the 100 TeV $pp$ collider. The sensitivities to probing new physics scales

of other nTGC operators are around (1–1.8) TeV at the LHC and (3.9–9.3) TeV at the 100 TeV $pp$ collider. We find that the sensitivities to the coefficients of $\mathcal{O}_{G-}$, $\tilde{\mathcal{O}}_{G-}$, and $\hat{h}^{\gamma}_{1,3}$ are significantly higher than that of the case by assuming the on-shell $Z\gamma$ final states [1].

Finally, we analyze the correlation contours (95% C.L.) between the sensitivities to the form factors of the off-shell nTGC vertex $Z^*\gamma V^*$, as shown in Fig. 2 [23]. We find that the behavior of the $\hat{h}_4 - \hat{h}^Z_3$ correlation is similar to that of their on-shell counterparts $h_4$ and $h^Z_3$ [1]. Specifically, the $\hat{h}_4 - \hat{h}^V_3$ correlation is rather small, while the sensitivity to $\hat{h}^{\gamma}_3$ is much greater than that to $h^{\gamma}_{31}$, especially at the 100 TeV $pp$ collider. On the other hand, the correlation between $\hat{h}^Z_3$ and $\hat{h}^{\gamma}_3$ is large at the LHC, but almost invisible at the 100 TeV $pp$ collider. This is because the $\hat{h}^{\gamma}_3$ contribution is enhanced by the off-shell momentum square $q_1^2/M_Z^2$ of $Z^*$ and $\hat{h}^Z_3$ is not, which makes their correlation suppressed by $1/\sqrt{q_1^2}$. At the LHC, the on- and off-shell contributions to $h^{\gamma}_3$ are comparable, so the $\hat{h}^Z_3 - \hat{h}^{\gamma}_3$ correlation can be significant; whereas their correlation is much suppressed by $1/\sqrt{q_1^2}$ at the 100 TeV $pp$ collider and becomes nearly invisible.

*Conclusions.* In this Letter, we have demonstrated that the reaction $pp(q\bar{q}) \to Z^*\gamma \to \nu\bar{\nu}\gamma$ can probe sensitively both the CPC and CPV nTGCs at the LHC and at the projected 100 TeV $pp$ colliders. It has comparable sensitivities to the on-shell production channels $pp(q\bar{q}) \to Z\gamma$ with $Z \to \ell^+\ell^-$ [1]. We formulated both CPC and CPV doubly off-shell nTGC vertices $Z^*\gamma V^*$ that are compatible with the electroweak $\mathrm{SU}(2) \otimes \mathrm{U}(1)$ gauge symmetry of the SMEFT at dimension eight. We found that the conventional form factor formulas of doubly on-shell vertices $Z\gamma V^*$ [7] are inadequate, and the conventional form factors $(h^V_3, h^V_4)$ and $(h^V_1, h^V_2)$ must be replaced by the new form factors $(h^{\gamma}_{31}, \hat{h}^V_3, \hat{h}_4)$ and $(h^{\gamma}_{11}, \hat{h}^V_1, \hat{h}_2)$ as in Eqs. (5) and (7).

We have presented the prospective sensitivity reaches on the nTGC form factors $\hat{h}^V_j$ at the LHC and the 100 TeV $pp$ collider in Table I and the sensitivity reaches on the new physics scales $\Lambda_j$ of the dimension-8 nTGC operators in Table II. We found in Table I that including the off-shell decays $Z^* \to \nu\bar{\nu}$ can increase the sensitivity reaches on $(\hat{h}^{\gamma}_3, \hat{h}^{\gamma}_1)$ by 50%–60% at the LHC and by a factor of $O(10)$ at the 100 TeV $pp$ collider. We present in Fig. 2 the correlations between the sensitivities to each pair of nTGC form factors.

We quantitatively compared our new predictions of the CPC nTGCs with the existing ATLAS measurements [5] as in Eqs. (13) and (14). This demonstrates that for the $\nu\bar{\nu}\gamma$ channel the LHC sensitivity reaches on the nTGC form factors $\hat{h}^{\gamma}_3$ and $\hat{h}_4$ differ significantly from the ATLAS results (using the conventional $Z\gamma V^*$ formulas).

This work establishes a new perspective for ongoing experimental probes of the new physics in nTGCs at the LHC and the projected 100 TeV $pp$ colliders. We look forward to continuing the fruitful cooperation with the LHC experimental groups, extending their ongoing nTGC analyses by using our new nTGC formulation.

*Acknowledgments.* We thank our ATLAS colleague Shu Li for discussing the ATLAS analyses and the estimate of their detection efficiency. The work of J. E. was supported in part by United Kingdom STFC Grant No. ST/T000759/1 and in part by the SJTU distinguished visiting fellow program. The work of H. J. H. and R. Q. X. was supported in part by the National NSF of China (under Grants No. 11835005 and No. 12175136). R. Q. X. has been supported by an International Postdoctoral Exchange Fellowship.

[1] J. Ellis, H.-J. He, and R.-Q. Xiao, Phys. Rev. D **107**, 035005 (2023).
[2] J. Ellis, H.-J. He, and R.-Q. Xiao, Sci. China (Phys. Mech. Astron.) **64**, 221062 (2021).
[3] J. Ellis, S.-f. Ge, H.-J. He, and R.-Q. Xiao, Chin. Phys. C **44**, 063106 (2020).
[4] V. Khachatryan *et al.* (CMS Collaboration), Phys. Lett. B **760**, 448 (2016).
[5] M. Aaboud *et al.* (ATLAS Collaboration), J. High Energy Phys. 12 (2018) 010.
[6] For example, S. Jahedi, arXiv:2305.11266; S. Spor, E. Gurkanli, and M. Köksal, arXiv:2302.08245; S. Jahedi and J. Lahiri, J. High Energy Phys. 04 (2023) 085; S. Spor, Nucl. Phys. **B991**, 116198 (2023); A. Senol, S. Spor, E. Gurkanli, V. Cetinkaya, H. Denizli, and M. Köksal, Eur. Phys. J. Plus **137**, 1354 (2022); Q. Fu, J. C. Yang, C. X. Yue, and Y. C. Guo, Nucl. Phys. **B972**, 115543 (2021); A. Biekötter, P. Gregg, F. Krauss, and M. Schönherr, Phys. Lett. B **817**, 136311 (2021); A. Senol, H. Denizli, A. Yilmaz, I. Turk Cakir, K. Y. Oyulmaz, O. Karadeniz, and O. Cakir, Nucl. Phys. **B935**, 365 (2018); R. Rahaman and R. K. Singh, Eur. Phys. J. C **77**, 521 (2017); **76**, 539 (2016).
[7] G. J. Gounaris, J. Layssac, and F. M. Renard, Phys. Rev. D **61**, 073013 (2000); **62**, 073012 (2000); **65**, 017302 (2001).
[8] C. Degrande, J. High Energy Phys. 02 (2014) 101.
[9] For reviews, see J. Ellis in *The Conference Proceedings of "Beyond Standard Model: From Theory to Experiment"*

*(BSM-2021), Zewail City, Egypt, 2021* (2021), 10.31526/ACP.BSM-2021.16; I. Brivio and M. Trott, Phys. Rep. **793**, 1 (2019).

[10] B. Grzadkowski, M. Iskrzynski, M. Misiak, and J. Rosiek, J. High Energy Phys. 10 (2010) 085 and references therein.

[11] See, e.g., J. Ellis, V. Sanz, and T. You, J. High Energy Phys. 07 (2014) 036; 03 (2015) 157; H.-J. He, J. Ren, and W. Yao, Phys. Rev. D **93**, 015003 (2016); J. Ellis and T. You, J. High Energy Phys. 03 (2016) 089; S.-F. Ge, H.-J. He, and R.-Q. Xiao, J. High Energy Phys. 10 (2016) 007; J. de Blas, M. Ciuchini, E. Franco, S. Mishima, M. Pierini, L. Reina, and L. Silvestrini, J. High Energy Phys. 12 (2016) 135; F. Ferreira, B. Fuks, V. Sanz, and D. Sengupta, Eur. Phys. J. C **77**, 675 (2017) J. Ellis, P. Roloff, V. Sanz, and T. You, J. High Energy Phys. 05 (2017) 096; G. Durieux, C. Grojean, J. Gu, and K. Wang, J. High Energy Phys. 09 (2017) 014; T. Barklow, K. Fujii, S. Jung, R. Karl, J. List, T. Ogawa, M. E. Peskin, and J. Tian, Phys. Rev. D **97**, 053003 (2018); C. W. Murphy, Phys. Rev. D **97**, 015007 (2018); J. Ellis, C. W. Murphy, V. Sanz, and T. You, J. High Energy Phys. 06 (2018) 146; G. N. Remmen and N. L. Rodd, J. High Energy Phys. 12 (2019) 032; A. Gutierrez-Rodriguez, M. Koksal, A. A. Billur, and M. A. Hernandez-Ruiz, J. Phys. G **47**, 055005 (2020); M. Koksal, A. A. Billur, A. Gutierrez-Rodriguez, and M. A. Hernandez-Ruiz, Phys. Lett. B **808**, 135661 (2020); J. Ellis, M. Madigan, K. Mimasu, V. Sanz, and T. You, J. High Energy Phys. 04 (2021) 279 and references therein.

[12] We emphasize that the conventional electroweak form factor formulation imposes only the residual U(1) gauge symmetry of QED, and is in general *incompatible* with the SMEFT framework, which takes into account the full $\mathrm{SU}(2) \otimes \mathrm{U}(1)$ electroweak gauge symmetry of the SM. We stress that it is important to match precisely the form factors with the corresponding SMEFT operators in the broken phase, which can place additional nontrivial constraints on the structure of the form factors as a result of the spontaneous electroweak symmetry breaking of the SM. We demonstrate this point for our correct formulation of both the CPC and CPV nTGC form factors in the second section and in the Supplemental Material [14].

[13] H.-L. Li, Z. Ren, J. Shu, M.-L. Xiao, J.-H. Yu, and Y.-H. Zheng, Phys. Rev. D **104**, 015026 (2021); C. W. Murphy, J. High Energy Phys. 10 (2020) 174.

[14] See Supplemental Material at http://link.aps.org/supplemental/10.1103/PhysRevD.108.L111704, where we first present a general Lagrangian-level formulation of the fully off-shell form factors of $Z^*\gamma^*V^*$ $(V = Z, \gamma)$ from matching the corresponding dimension-8 operators in the electroweak broken phase, including both the CP-conserving (CPC) and CP-violating (CPV) contributions. Then, we present the cross sections for CPC and CPV nTGC contributions which are used for the analyses in the main text. Finally, we derive the unitarity constraints on the CPC and CPV nTGCs, and demonstrate that they are much weaker than our current collider bounds (shown in Tables I and II of the main text) and thus do not affect our collider analyses.

[15] We note that the CMS [4] and ATLAS [5] Collaborations also measured the CPC nTGC form factor $h_4^V$ using the conventional formula, which gives rise to unphysically large high-energy behavior [1,14].

[16] For a comprehensive review, see H. J. He, Y. P. Kuang, and C. P. Yuan, Report No. DESY-97-056 and arXiv:hep-ph/9704276; see also H. J. He and W. B. Kilgore, Phys. Rev. D **55**, 1515 (1997); H. J. He, Y. P. Kuang, and C. P. Yuan, Phys. Rev. D **51**, 6463 (1995); **55**, 3038 (1997); H. J. He, Y. P. Kuang, and X. Li, Phys. Lett. B **329**, 278 (1994); Phys. Rev. D **49**, 4842 (1994); Phys. Rev. Lett. **69**, 2619 (1992) and references therein.

[17] We observe that by matching the nTGC form factors with the corresponding dimension-8 operators of the SMEFT, the $(h_{11}^\gamma, h_{31}^\gamma)$ and $(\hat{h}_1^Z, \hat{h}_3^Z)$ form factors arise as a consequence of spontaneous electroweak symmetry breaking and would vanish if $\langle H \rangle = 0$. We also note that $\hat{h}_{1,3}^\gamma$ and $\hat{h}_{2,4}$ arise from the electroweak rotation of the $BW^3W^3$ vertex, so the $\hat{h}_{3,1}^\gamma$ terms in Eqs. (5a) and (7a) would vanish if $s_W = 0$.

[18] In principle, the partonic center-of-mass energy $\sqrt{\hat{s}}$ can be determined by measuring the invariant mass of the observable final-state particles. The ATLAS measurements of $M_{\ell\ell\gamma}$ during the LHC run 2 reached around 3 TeV. Accordingly, for the analysis of $Z^*\gamma(\nu\bar{\nu}\gamma)$ production, the relevant energy range is $\sqrt{\hat{s}} < 3$ TeV for the LHC and $\sqrt{\hat{s}} < 23$ TeV for the 100 TeV $pp$ collider.

[19] H. L. Lai *et al.* (CTEQ Collaboration), Eur. Phys. J. C **12**, 375 (2000); T. J. Hou *et al.* (CTEQ Collaboration), Phys. Rev. D **103**, 014013 (2021).

[20] We find that the situation is different for probing the nTGCs at high-energy $e^+e^-$ colliders [2,3], where the interference contribution can dominate over the squared contribution. In addition, imposing the inelastic unitarity condition [21], we have derived the perturbative unitarity bounds on the cutoff scales $\Lambda_j$ and the form factors $h_j^V$ in the Supplemental Material [14]. We have verified that these bounds are much weaker than our current collider bounds in the third section and thus do not affect our collider analyses.

[21] D. A. Dicus and H.-J. He, Phys. Rev. D **71**, 093009 (2005); Phys. Rev. Lett. **94**, 221802 (2005).

[22] G. Cowan, K. Cranmer, E. Gross, and O. Vitells, Eur. Phys. J. C **71**, 1554 (2011).From this literature, for the given signal events $S$ and background events $B$, the statistical significance under the background-with-signal hypothesis is given by

$$\mathcal{Z} = \sqrt{2\left(B \ln \frac{B}{B+S} + S\right)},$$

with which we obtain the formula (12) in the main text.

[23] We also note that no correlation exists between the CPC and CPV nTGCs because their amplitudes only differ by $\pm i$. Finally, correlations among $\hat{h}_2$, $\hat{h}_1^Z$, $\hat{h}_1^\gamma$, and $h_{11}^\gamma$ are similar to those of the corresponding CPC nTGCs, because the squared term $\sigma_2$ dominates the signal cross section at the LHC and at the 100 TeV $pp$ collider.